

Publications with LPKF equipment

Selection of internationally published scientific articles using LPKF equipment

November 2022



TOC: page, system, application

3 [PL U3: Soft Robots for Drug Delivery](#)

4 [PL U4: Implantable Photometry System](#)

5 [PL U4: Wearable Biosensor in Pediatric Care](#)

6 [PL U4: Implantable Osseosurface Biosensor](#)

7 [PL U4: Airline Point-of-Care System](#)

8 [PL U4: In Body Bio-resorbable Batteries](#)

9 [PL R: Programmable 3D Metamaterials](#)

10 [PL R: Wireless Implantable O₂ Measurement Probe](#)

11 [PL S: Electrocaloric Cooling](#)

12 [PM S100 Textronic RFID Transponder](#)

13 [PM S103: Dual-band mm-Wave Mobile Antenna](#)

14 [PL S62 & PL S: Triple-band 6G Antenna](#)

On-demand anchoring of wireless soft miniature robots on soft surfaces

Untethered soft miniature robots capable of accessing hard-to-reach regions can enable new, disruptive, and minimally invasive medical procedures. However, once the control input is removed, these robots easily move from their target location because of the dynamic motion of body tissues or fluids, thereby restricting their use in many long-term medical applications. To overcome this, we propose a wireless spring-preloaded barbed needle release mechanism, which can provide up to 1.6 N of force to drive a barbed needle into soft tissues to allow robust on-demand anchoring on three-dimensional (3D) surfaces. The mechanism is wirelessly triggered using a radio-frequency remote...

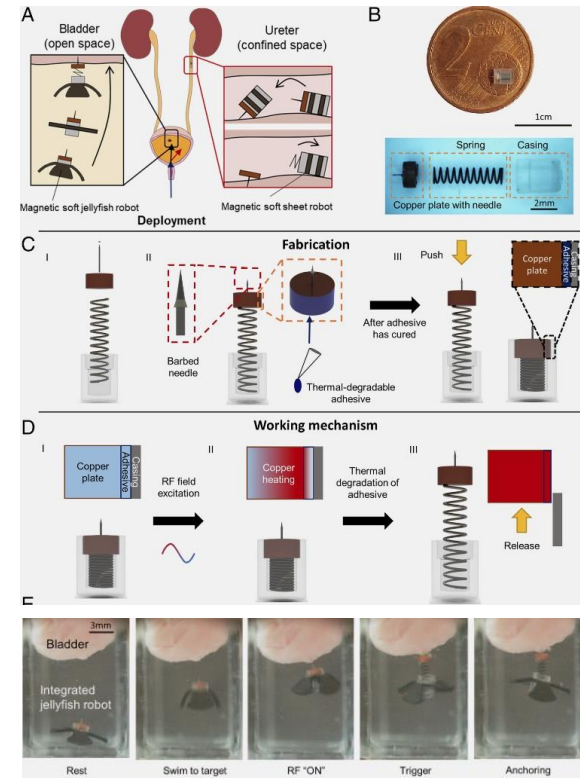
Wireless Magnetic Soft Millirobot Fabrication.

The soft millirobots were fabricated with a method described previously (10). Briefly, Scotch tape (840, 3M) was first placed along the sides of an acrylic sheet. The number of layers placed determined the thickness of the robot. Neodymium-iron-boron (NdFeB) magnetic microparticles (MQP-15-7, Magnequench) were mixed with platinum-catalyzed silicone (Ecoflex 00-10, Smooth-On Inc.) in a 1:1 mass ratio, degassed for 5 min, poured on the acrylic sheet, and evened out with a razor blade. The sample was then left to cure on a hot plate at 65 °C for 1 h. After the sample had cured, it was laser cut (**ProtoLaser U3**, LPKF Laser & Electronics AG) to the desired dimensions.

Physical Intelligence Department, Max Planck Institute for Intelligent Systems, 70569 Stuttgart, Germany

<https://www.pnas.org/doi/10.1073/pnas.2207767119>

Wireless medical robots, soft robots, miniature robots, surface anchoring



Wireless, battery-free subdermally implantable photometry systems for chronic recording of neural dynamics

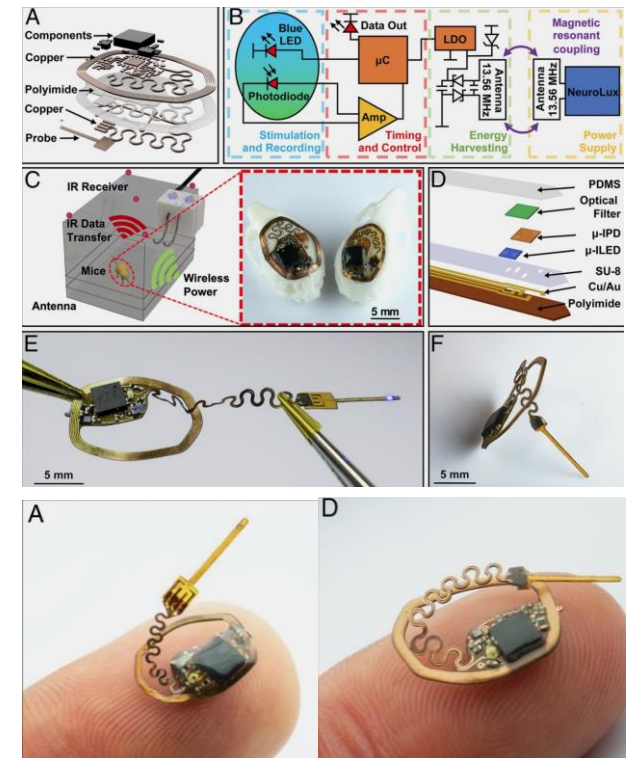
Recording cell-specific neuronal activity while monitoring behaviors of freely moving subjects can provide some of the most significant insights into brain function. Current means for monitoring calcium dynamics in genetically targeted populations of neurons rely on delivery of light and recording of fluorescent signals through optical fibers that can reduce subject mobility, induce motion artifacts, and limit experimental paradigms to isolated subjects in open, two-dimensional (2D) spaces. Wireless alternatives eliminate constraints associated with optical fibers, but their use of head stages with batteries adds bulk and weight that can affect behaviors, with limited ...

Flexible Circuit Fabrication: Pyralux (AP8535R; constituent layers, 17.5- μm copper, 75- μm polyimide, and 17.5- μm copper) served as a substrate. The copper traces, vias, and device outline were defined using a UV (355-nm) laser ablation system (LPKF; **Protolaser U4**) with subsequent ultrasonic cleaning (Vevor; Commercial Ultrasonic Cleaner 2L) for 10 min in flux (Superior Flux and Manufacturing Company; Superior #71) and 1 min in isopropyl alcohol (IPA) (MG Chemicals) and rinsing with deionized (DI) water to remove oxidation and organic residue. Via connections were established manually with copper wire (100 μm) and low-temperature solder (Chip Quik; TS391LT).

Department of Biomedical Engineering, The University of Arizona, Tucson, AZ 85721

<https://www.pnas.org/doi/10.1073/pnas.1920073117>

Photometry, neural dynamics, genetically encoded calcium indicator

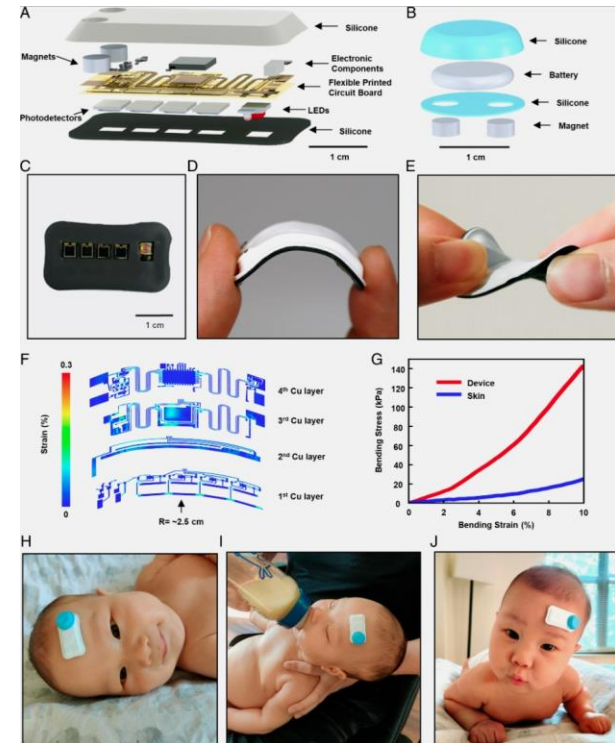


A wireless, skin-interfaced biosensor for cerebral hemodynamic monitoring in pediatric care

The standard of clinical care in many pediatric and neonatal neurocritical care units involves continuous monitoring of cerebral hemodynamics using hard-wired devices that physically adhere to the skin and connect to base stations that commonly mount on an adjacent wall or stand. Risks of iatrogenic skin injuries associated with adhesives that bond such systems to the skin and entanglements of the patients and/or the healthcare professionals with the wires can impede clinical procedures and natural movements that are critical to the care, development, and recovery of pediatric patients. This paper presents a wireless, miniaturized, and mechanically soft, flexible device that supports measurements quantitatively comparable to existing clinical standards.

Device Fabrication: Fabrication began with a 25- μm -thick polyimide sheet, with 12- μm -thick Cu on both sides (AP7164R; Dupont) and outlined using an ultraviolet laser cutter (ProtoLaser U4; LPKF). Electronic and sensor components, along with a pair of magnets (5862K13; McMaster Carr), were bonded to the circuit board by solder paste (TS391LT; Chip Quik). The board was folded and encapsulated within thin layers of medical-grade silicone (Silbione RTV 4420; Elkem) defined by an aluminum mold and subsequently filled with soft silicone (Ecoflex 00-10; Smooth-On). The final shape was outlined using a CO2 laser cutter (VLS3.5; Universal Laser).

wearable electronics, near-infrared spectroscopy, bioelectronics, cerebral hemodynamics



Querrey Simpson Institute for Bioelectronics, Northwestern University, Chicago, IL 60208

<https://arxiv.org/pdf/2105.10611.pdf>



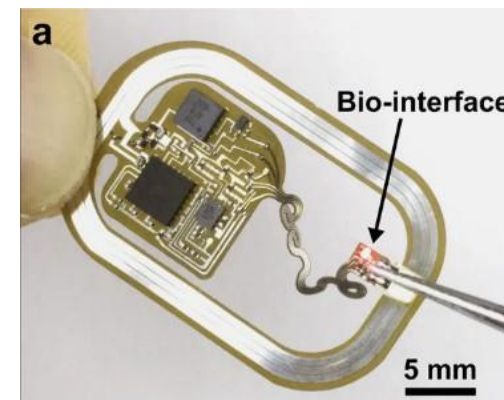
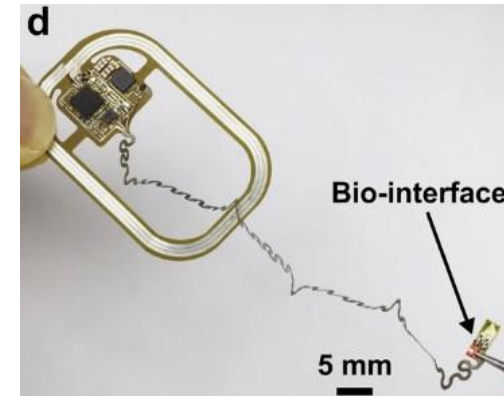
Osseosurface electronics—thin, wireless, battery-free and multimodal musculoskeletal biointerfaces

Bioelectronic interfaces have been extensively investigated in recent years and advances in technology derived from these tools, such as soft and ultrathin sensors, now offer the opportunity to interface with parts of the body that were largely unexplored due to the lack of suitable tools. The musculoskeletal system is an understudied area where these new technologies can result in advanced capabilities. Bones as a sensor and stimulation location offer tremendous advantages for chronic biointerfaces because devices can be permanently bonded and provide stable optical, electromagnetic, and mechanical impedance over the course of years. Here we introduce a new ...

Device fabrication: Flexible circuitries were fabricated by UV (355 nm) laser ablation (**ProtoLaser U4**, LKPF, Germany) using a sheet of copper-clad polyimide foil (Dupont, Pyralux AP8535R, copper /Polyimide/copper, 17.5 μm /75 μm /17.5 μm) as substrate. Subsequent sonication in solder flux and isopropanol removed the surface oxides formed during laser ablation. Surface-mount components, including passive components such as resistors (0201, 0.6 mm \times 0.3 mm), capacitors, Schottky diodes (Skyworks Inc.), Zener diodes (Comchip Technology Corp., 5.6 V), μ -ILED (red, ES-AEHRAX10, EPSTAR), and NTC thermistor (NTCG064EF104FTBX, TDK), as well as active components such as MOSFET (PMZ130UNE, Nexperia), low-dropout linear regulators (LDO, TCR2DG18, Toshiba), ...
Department of Biomedical Engineering, University of Arizona, Tucson, AZ 85721, USA

<https://www.nature.com/articles/s41467-021-27003-2>

Osseosurface electronics,
biointerface, biosensors



Airline Point-of-Care System on Seat Belt for Hybrid Physiological Signal Monitoring

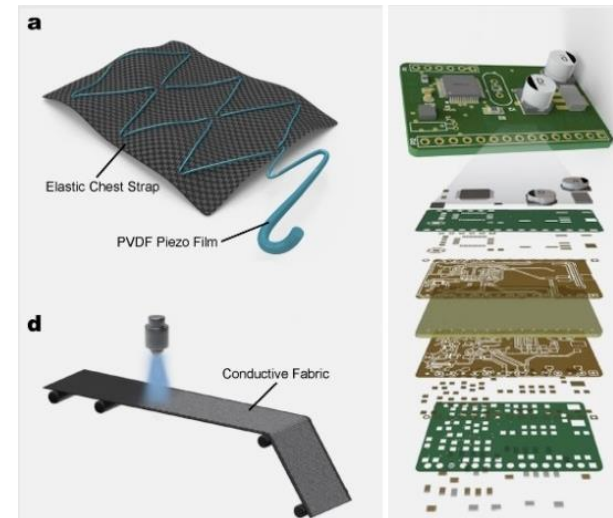
With a focus on disease prevention and health promotion, a reactive and disease-centric healthcare system is revolutionized to a point-of-care model by the application of wearable devices. The convenience and low cost made it possible for long-term monitoring of health problems in long-distance traveling such as flights. While most of the existing health monitoring systems on aircrafts are limited for pilots, point-of-care systems provide choices for passengers to enjoy healthcare at the same level. Here in this paper, an airline point-of-care system containing hybrid electrocardiogram (ECG), breathing, and motion signals detection is proposed. At the same time, we propose ...

The signal acquisition terminal consists of a controller box, a biomedical sensor, and an elastic chest strap, which enables 8 h of continuously monitoring. The extended monitoring time of the flexible electrode shows almost no influence on the signal sensitivity and the SNR. The collected ECG signal is processed by the circuit and sent to the microprocessor, and then transmitted to the computer through a Bluetooth module for further analysis and processing. The removable controller box contains a power supply, a communication module, a signal processing module, the main control chip, and the memory, which is integrated on a fast-prototyping PCB board that patterned using a UV laser system (LPKF; **Protolaser U4**), as shown in Figure 2c. Four electrode buttons are mounted on the elastic chest strap.

School of Life Science and Technology, Changchun University of Science and Technology, Changchun 130022, China

<https://www.mdpi.com/2072-666X/13/11/1880>

Point-of-Care, SAHS



High performance dual-electrolyte magnesium–iodine batteries that can harmlessly resorb in the environment or in the body

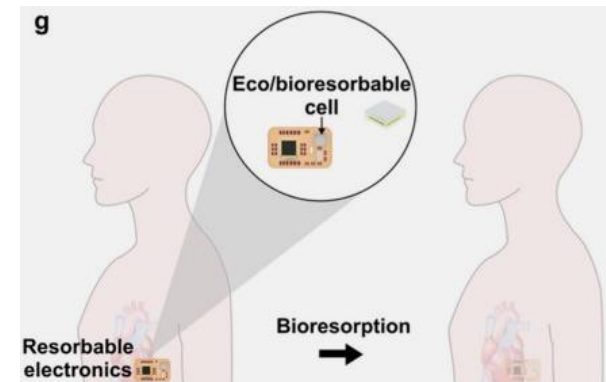
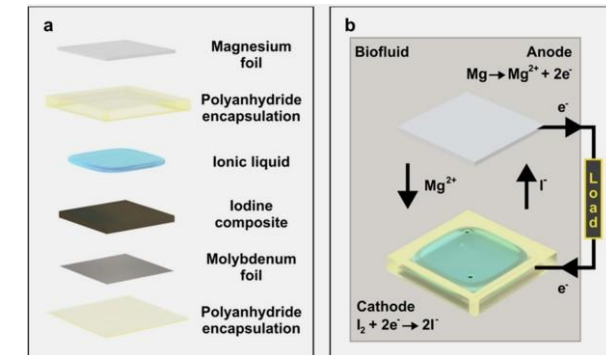
Batteries represent the dominant means for storing electrical energy, but many battery chemistries create waste streams that are difficult to manage, and most possess toxic components that limit their use in biomedical applications. Batteries constructed from materials capable of complete, harmless resorption into the environment or into living organisms after a desired period of operation bypass these disadvantages. However, previously reported eco/bioresorbable batteries offer low operating voltages and modest energy densities. Here, we introduce a magnesium–iodine chemistry and dual (ionic liquid/aqueous) electrolyte to overcome these limitations, enabling significant improvements

Fabrication of the eco/bioresorbable cells: The cells used metal foils Mo (15 mm thick) and Mg (200 mm thick) purchased from Alibaba, and Mo gauze (20 mesh) purchased from Alfa Aesar. An ultraviolet laser (**LPKF U4**) defined the shapes of the anodes and cathodes. Mixing 9 : 1 ball-milled iodine (Sigma) and super P (MTI) with 600 mL of 300 mg mL⁻¹ poly(D,L-lactide-co-glycolide) (PLGA) 65 : 35 Mw 40–75k (Sigma) in ethyl acetate and 800 mL of 3 wt% HMW chitosan in 1 M acetic acid within a planetary mixer (Thinky ARE-30; 10 min mix) formed a uniformly distributed slurry for the cathode. Positioning Mo foils/gauze in the trenches of a 3D printed mold, followed by orthogonally aligning a 3D printed spatula against the length of the foils, yielded 5 mm x 5 mm pockets to ...

Center for Bio-Integrated Electronics, Northwestern University, Evanston, IL, 60208, USA

<http://rogersgroup.northwestern.edu/files/2022/eestransbatt.pdf>

Bio-resorbable batteries, implantable batteries



Machine learning assisted design of shape-programmable 3D kirigami metamaterials

Kirigami-engineering has become an avenue for realizing multifunctional metamaterials that tap into the instability landscape of planar surfaces embedded with cuts. Recently, it has been shown that two-dimensional Kirigami motifs can unfurl a rich space of out-of-plane deformations, which are programmable and controllable across spatial scales. Notwithstanding Kirigami’s versatility, arriving at a cut layout that yields the desired functionality remains a challenge. Here, we introduce a comprehensive machine learning framework to shed light on the Kirigami design space and to rationally guide the design and control of Kirigami-based materials from the meta-atom to the metamaterial level.

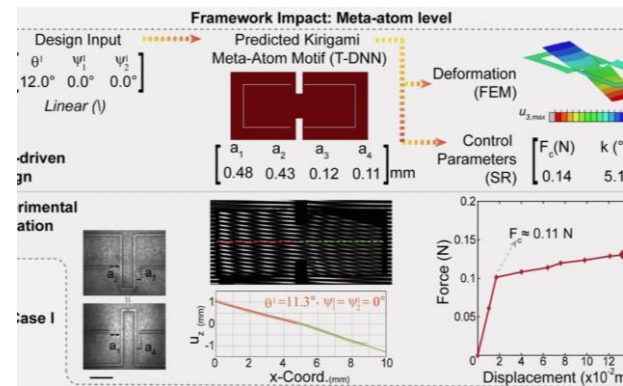
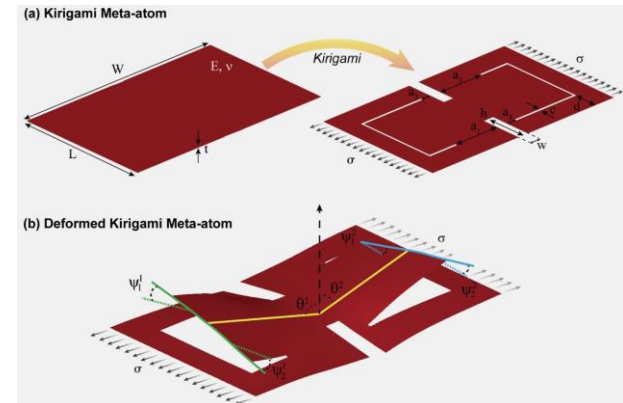
Fabrication

Kirigami meta-atoms, 1D and 2D arrays were fabricated using an LPKF **Protolaser R** laser cutter (LPKF Laser & Electronics, Tualatin, USA) housed in Northwestern University’s Micro/Nano Fabrication Facility. The substrate material was Kapton HN200 (Dupont, Wilmington, USA). Samples for Moire imaging were spray coated with white aerosol to allow for contrast.

Theoretical and Applied Mechanics, Northwestern University, Evanston, IL 60208, USA

<https://www.nature.com/articles/s41524-022-00873-w>

3D metadevices, programable kirigami



Wireless implantable optical probe for continuous monitoring of oxygen saturation in flaps and organ grafts

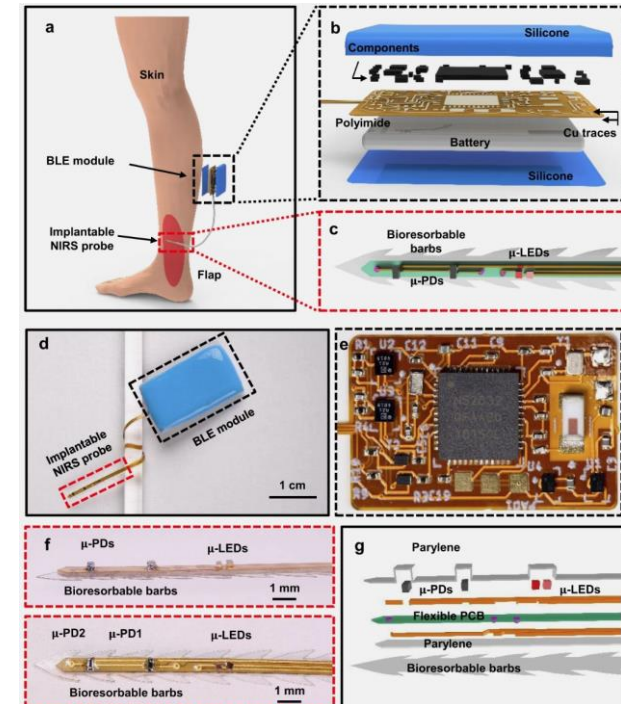
Continuous, real-time monitoring of perfusion after microsurgical free tissue transfer or solid organ allotransplantation procedures can facilitate early diagnosis of and intervention for anastomotic thrombosis. Current technologies including Doppler systems, cutaneous O₂-sensing probes, and fluorine magnetic resonance imaging methods are limited by their intermittent measurements, requirements for skilled personnel, indirect interfaces, and/or their tethered connections. This paper reports a wireless, miniaturized, minimally invasive near-infrared spectroscopic system designed for uninterrupted monitoring of local-tissue oxygenation. A bioresorbable barbed structure anchors ...

Preparation of bioresorbable barbs: The process began with dissolving Poly(D, L-lactide-co-glycolide) (PLGA, lactide: glycolide (50:50), mol wt 30,000–6000, Sigma–Aldrich/Millipore Sigma) with ethyl acetate at a concentration of 5% w/v. Drop casting 8 mL of the PLGA solution onto a 4 inch Si wafer with a self-assembled silane monolayer (trichloro(1H,1H,2H,2H-perfluorooctyl) silane, Sigma–Aldrich/Millipore Sigma), evaporating the solvent in a fume hood overnight, then baking at 70 °C for 2 h yielded PLGA film with thicknesses of ~100 μm. A laser cutter (**LPKF ProtoLaser R**) defined the outline of the PLGA barbs that attached to the backside of the probe using pressure by finger pressing and baking at 65–70 °C.

Department of Materials Science and Engineering, Northwestern University, Evanston, IL 60208, USA

<https://www.nature.com/articles/s41467-022-30594-z>

Bioresorbable, local tissue oxygenation measurement



Multifunctional Cantilevers as Working Elements in Solid-State Cooling Devices

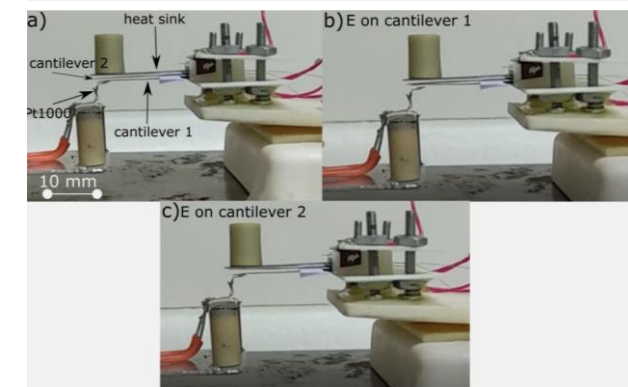
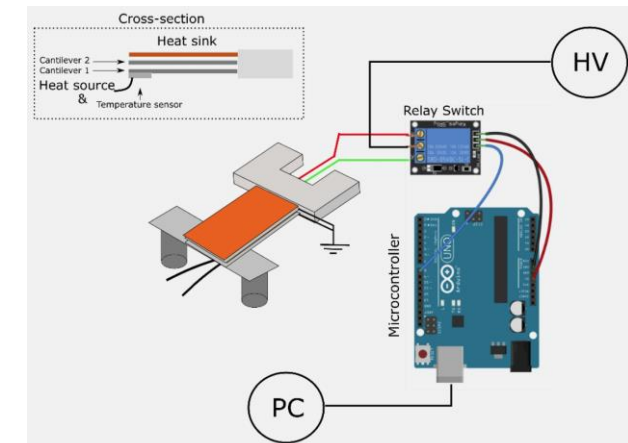
Despite the challenges of practical implementation, electrocaloric (EC) cooling remains a promising technology because of its good scalability and high efficiency. Here, we investigate the feasibility of an EC cooling device that couples the EC and electromechanical (EM) responses of a highly functionally, efficient, lead magnesium niobate ceramic material. We fabricated multifunctional cantilevers from this material and characterized their electrical, EM and EC properties. Two active cantilevers were stacked in a cascade structure, forming a proof-of-concept device, which was then analyzed in detail. The cooling effect was lower than the EC effect of the material itself, mainly ...

Fabrication: The cantilevers were prepared by tape casting the PMN tapes and screen printing the platinum electrodes according to the procedures described by Fulanović et al. [17]. The cantilevers consisted of a platinum layer sandwiched by two PMN layers. The green tapes were first fired at 450 °C for 5 h to burn out the organic solvents and then heated to 1200 °C, where they were sintered for 2 h. The sintered tapes were then laser-cut (LPKF ProtoLaser S, Garbsen, Germany) to specific dimensions (30 mm × 7 mm). The microstructure and thickness were analysed using a JSM-7600F scanning electron microscope (SEM, JEOL, Tokyo, Japan). The X-ray diffraction (XRD) data were recorded using a 1D detector (X’Celerator, PANalytical) and a diffractometer (X’Pert PRO MPD, PANalytical, Almelo,...

Jožef Stefan Institute, Jamova cesta 39, 1000 Ljubljana, Slovenia

<https://www.mdpi.com/2076-0825/10/3/58/htm>

electrocaloric response; electromechanical response; multifunctional materials; cooling

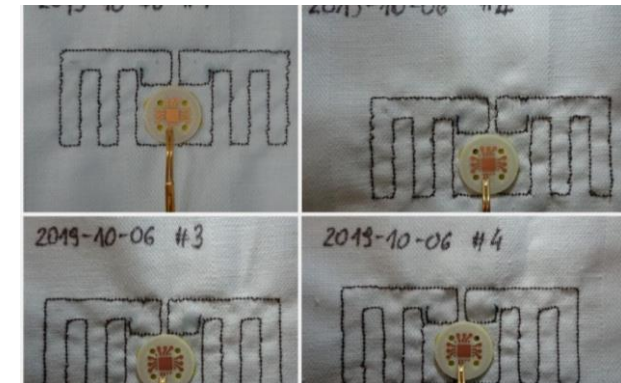
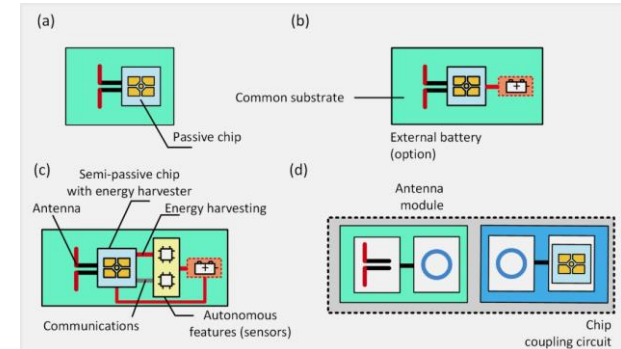


Textronic UHF RFID Transponder

In order to respond to the growing interest in radio frequency identification textile transponders, the authors propose a new approach to design radio frequency identification (RFID) devices by introducing the RFIDtex concept. The coupling system of inductive loops is implemented in the textronic structure with the RFID interface in order to split the transponder into two independently manufactured components. Then both modules can be easily integrated into the RFIDtex tag. The presented simulation and measurement results prove the concept of manufacturing a relatively small antenna in the form of a meandered dipole sewn in with a single thread, and further, that ...

RFID Transponder Manufacturing: Test samples of the elaborated RFIDtex transponder were made on the basis of the obtained numerical model (Figure 11). The antenna module of samples was manufactured on substrates that combine linen fabric and fleece, by using embroidery machine Brother INNOV-IS V3 (Brother Industries, Nagoya, Japan). In addition, the chip module was milled (footprint for the AMS SL900A chip) by using PCB plotter LPKF ProtoMat S100 (LPKF Laser & Electronics AG, Garbsen, Germany).

Smart textiles, RFID, textronic, Internet of Textile Things (IoTT)



Department of Electronic and Telecommunications Systems, Rzeszów University of Technology, Wincentego Pola 2, 35-959 Rzeszów, Poland

<https://www.mdpi.com/1424-8220/21/4/1093/htm>

A Compact Low-Profile Antenna for Millimeter-Wave 5G Mobile Phones

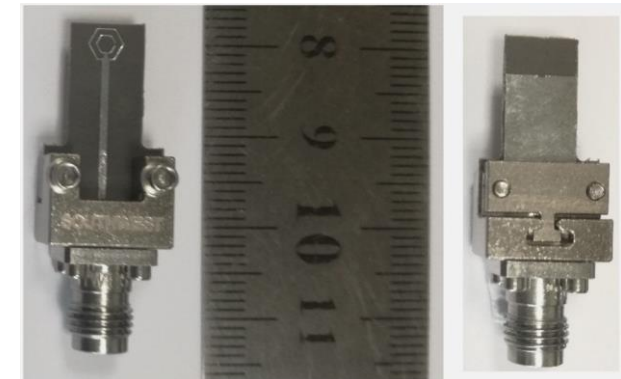
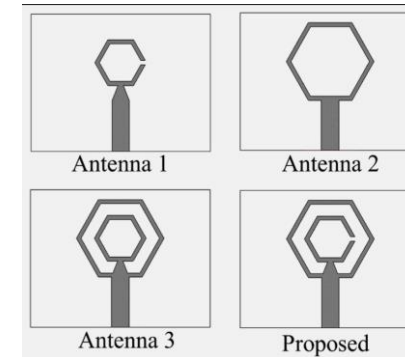
This paper presents a very low profile and simple antenna design for dual beam and dual-band operation to be employed in future 5G mobile phones operating in the millimeter-wave bands of 26.75–30.31 and 35.83–41.22 GHz. The two distinct resonances at 28 and 38 GHz are achieved using a meta-material-based structure consisting of a closed-ring resonator (CRR) and a split-ring resonator (SRR) by co-centrally combining two planar hexagonal rings; i.e., an inner split-ring resonator (SRR) and an outer closed-ring resonator (CRR). The antenna has a high gain of 4.5 dBi. The antenna also exhibits a dual-beam radiation pattern in one of its planes. The overall antenna...

The antenna was fabricated on Rogers 5880 board using an in-house standard PCB manufacturing facility (**LPKF S103**). The fabricated prototype was then fixed with a Southwest RF connector as shown in Figure 8. The feed line was extended for easy mounting of the antenna onto the connector. The antenna was tested for radiation patterns in our in-house anechoic chamber facility (range: 800 MHz–40 GHz). The simulated and measured reflection coefficients (S11) are shown in Figure 9. The simulated S11 showed that the lower band ranged from 26.983 GHz to 29.814 GHz and the upper band from 34.29 GHz to 42.206 GHz. The measured S11 followed the same trend and showed two distinct bands; i.e., at 26.75–30.31 GHz and 35.83–41.22 GHz. Thus, the desired bands of 28 GHz...

School of Electrical Engineering and Computer Science, National University of Sciences and Technology, Islamabad 44000, Pakistan

<https://www.mdpi.com/2079-9292/11/19/3256/htm>

5G; millimeter-wave; dual-band;
28/38 GHz; dual-beam; metamaterial



Design of Triple-Band (DSRC, 5G, 6G) Antenna for Autonomous Vehicle Telematics

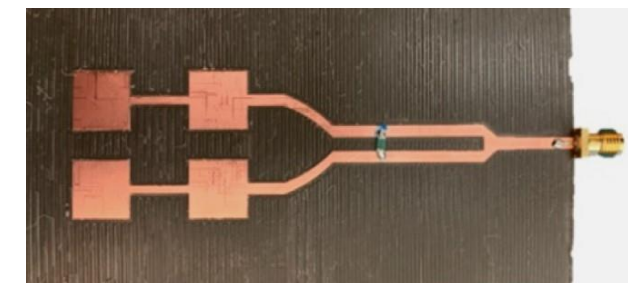
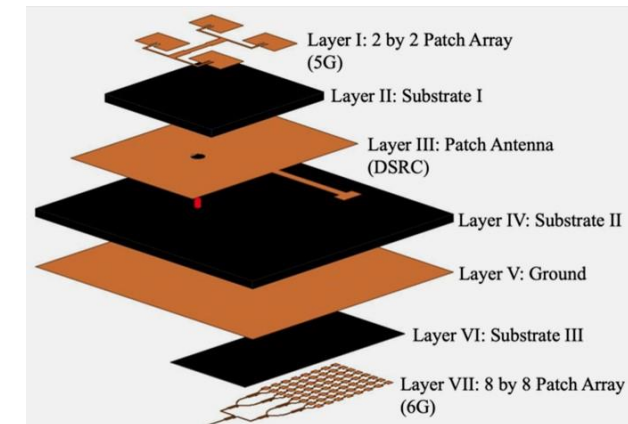
A triple-band stacked-patch antenna covering dedicated short-range communication (DSRC), fifth-generation (5G) millimeter-wave, and sixth-generation (6G) millimeter-wave frequency bands is reported for autonomous vehicles telematics applications. To show the effectiveness of the developed antenna, the antenna performances, such as the S-parameter, realized gain at boresight, and radiation patterns were simulated and measured for DSRC and 5G, and only simulated for 6G. The simulated results show good agreement with the measured results. The results show that the developed triple-band antenna can cover all three bands with high peak realized gains of 6.87 dBi, ...

Antenna Fabrication and Measured Results: Figure 15 shows the fabricated dual-band DSRC+5G antenna array constructed according to the specifications in Table 1 and designs in Figure 1 and Figure 2. The top two-by-two 5G inset-fed patch array and bottom DSRC patch antenna were built using an in-house precision milling machine (**LPKF ProtoMat S62 and ProtoLaser S**). The 2.92 mm SMA connectors from Southwest Microwave (1012-16SF and 1092-03A-6) were used for both port I (5G) and II (DSRC), respectively. A vector network analyzer (VNA: Agilent E8361C PNA) was used to characterize S-parameters of the fabricated dual-band antenna. The VNA can measure from 10 MHz to 67 GHz with 94 dB of dynamic range. We measured the radiation patterns at the DSRC ...

Department of Electrical and Computer Engineering, The University of Alabama, Tuscaloosa, AL 35487, USA

<https://www.mdpi.com/2079-9292/11/16/2523/htm>

patch antenna array; telematics;
triple-frequency



Check for your sources for articles and papers

www.nature.com

www.researchgate.net

www.mdpi.com

www.pnas.org

<https://advances.sciencemag.org/>

[Springer - International Publisher Science, Technology, Medicine](#)

[Open Access Scientific Reports , OMICS International \(omicsonline.org\)](#)

[LPKF Knowledge center](#)

[Contact LPKF](#)